Journal of Organometallic Chemistry 694 (2009) 2029–2036

Contents lists available at ScienceDirect

Journal of Organometallic Chemistry

journal homepage: www.elsevier.com/locate/jorganchem

Behaviour of $[RuClCp(mPTA)_2](OSO_2CF_3)_2$ in water *vs.* the pH: Synthesis and characterisation of $[RuCpX(mPTA)_2](OSO_2CF_3)_n$, X = ($H_2O$-κ*O*, DMSO-κ*S*, *n* = 3; OH^--κ*O*, *n* = 2) (mPTA = N-methyl-1,3,5-triaza-7-phosphaadamantane)

Beatriz González [a], Pablo Lorenzo-Luis [a,*], Pedro Gili [a], Antonio Romerosa [b,*], Manuel Serrano-Ruiz [b]

[a] Departamento de Química Inorgánica, Facultad de Química, Universidad de La Laguna, La Laguna, Tenerife, Spain
[b] Área de Química Inorgánica, Facultad de Ciencias, Universidad de Almería, Almería, 04120, Spain

ARTICLE INFO

Article history:
Received 8 January 2009
Received in revised form 28 January 2009
Accepted 28 January 2009
Available online 5 February 2009

Keywords:
Ruthenium complexes
Aquo-soluble metal complexes
mPTA
Water reactivity

ABSTRACT

The behaviour of $[RuClCp(mPTA)_2](OSO_2CF_3)_2$ (**1**) in water solution *vs.* the pH was studied. Complex **1** is stable in neutral and acidic water solution while in basic water solution another complex, $[RuCp(OH\text{-}\kappa O)(mPTA)_2](OSO_2CF_3)_2\cdot(C_4H_{10}O)$ (**2**), is obtained. Complexes $[RuCp(mPTA)_2(L)]\cdot X_n$ (L = H_2O-κ*O*, X = $^-OSO_2CF_3$, *n* = 3 (**3**); L = Cl, X = BF_4^-, n = 2 (**4**); L = DMSO-κ*S*, X = $^-OSO_2CF_3$, *n* = 3 (**5**)) were also obtained. All presented complexes were characterised by IR and multinuclear (^1H, $^{13}C\{^1H\}$, $^{19}F\{^1H\}$and $^{31}P\{^1H\}$) NMR spectroscopy. Improved synthesis for **1**, the thermal analysis of complexes **1–3** and the crystal structure of the complexes **1** and **5** are also presented.

1. Introduction

The aquo-soluble ruthenium(II) complexes containing water-soluble phosphine ligands have received a great deal of attention in recent years [1]. Water is employed more and more often as a medium for the synthesis of organic compounds and study of their transformations. This approach is advantageous for some important reasons: water is abundant, environmentally benign [2] and reported to be actively involved in a variety of reactions by coordinating to a metal centre and/or by proton transfer [3].

Among aminophosphine ligands, the air-stable, water-soluble, heterocyclic phosphine 1,3,5-triaza-7-phosphaadamantane (PTA) has received much attention in recent years as a ligand for the synthesis of water-soluble metal complexes which find use in such areas as medicine, catalysis, photo-luminescence, etc. [4,5]. Recently our group has presented the first water-soluble and air-stable heterobimetallic polymeric structure containing $[CpRuCNRuCp]^+$ and $[Au(CN)_4]^-$ bridged by PTA through a P,N coordination mode. This complex displays gel-like properties in water, specifically a thermally controlled volume transition [9]. A number of aqua-soluble phosphines with the PTA cage modified by cleavage of C–N or C–P bonds have appeared in literature over the years [6]. We have reported the synthesis of $mPTA(OSO_2CF_3)$ (N-methyl-1,3,5-triaza-7-phosphaadamantane) [7] and its three new derivatives: dmPTA (N,N′-dimethyl-1,3,5-triaza-7-phosphaadamantane), dmoPTA (3,7-dimethyl-1,3,5-triaza-5-phosphabicyclo[3.3.1]nonane and Hdmo PTA (3,7-H-3,7-dimethyl-1,3,7-triaza-5-phosphabicyclo[3.3.1]nonane) [8]. These ligands are used to obtain new complexes such as $[RuClCp(PPh_3)\text{-}\mu\text{-}dmoPTA\text{-}1\kappa P{:}2\kappa^2\,N,N'\text{-}Co(acac\text{-}\kappa^2 O,O')_2]$ which catalyses the isomerization of enols to enones [8].

The complex $[RuClCp(mPTA)_2]\cdot(OSO_2CF_3)_2$ (**1**) [7] is believed to be a promising water-soluble catalyst as parent complexes have shown activity for hydrogenation of olefins in water [10]. The difficulties of obtaining this complex in substantial amount have limited study of its properties. In this paper, we present new procedures, which allow obtaining **1** with a high yield and assessment of its behaviour in water *vs.* the pH [11].

2. Results and discussion

2.1. Synthesis and behaviour in water of $[RuClCp(mPTA)_2](OSO_2CF_3)_2$ (*1*)

The complex $[RuClCp(mPTA)_2](OSO_2CF_3)_2$ (1) was previously synthesised [7] by reaction of $RuCl_3\cdot xH_2O$ with freshly cracked cyclopentadiene (Cp) and $mPTA(OSO_2CF_3)$ in EtOH in low yield (~12.9%). We have tried to use two new alternative procedures for obtaining 1 from the parent complex $[RuClCp(PPh_3)_2]$ [7], which are shown in Scheme 1. Reaction of $[RuClCp(PPh_3)_2]$ with two equivalents of PTA in refluxing toluene results in the complex

* Corresponding authors.
E-mail addresses: plorenzo@ull.es (P. Lorenzo-Luis), romerosa@ual.es (A. Romerosa).

0022-328X/$ - see front matter © 2009 Elsevier B.V. All rights reserved.
doi:10.1016/j.jorganchem.2009.01.050

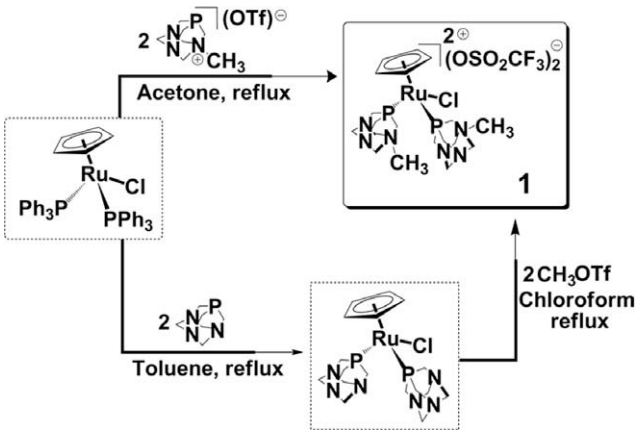

Scheme 1. Synthesis of **1**.

[RuClCp(PTA)$_2$] [12] that is further selectively methylated on the N_{PTA} by $CH_3OSO_2CF_3$ in refluxing chloroform. The complex 1 is obtained by this procedure from [RuClCp(PTA)$_2$] with 74% yield but from [RuClCp(PPh_3)$_2$] the yield is 39.6%. A more convenient synthetic strategy consists in the substitution of two PPh_3 groups in [RuClCp(PPh_3)$_2$] by two mPTA(OSO_2CF_3) in acetone. The composition of the final product obtained by this reaction depends on the reactant concentration. In adequate experimental conditions complex 1 is obtained in one step with a yield of 64% while a mixture of complexes [RuClCp(mPTA)$_2$](OSO_2CF_3)$_2$ (**1**) and [RuClCp (mPTA)(PPh_3)](OSO_2CF_3) (**1a**) is obtained if concentrations of the reactants are lower than the optimal ones.

It is important to stress that the reaction of **1a** with mPTA (OSO_2CF_3) in acetone did not give rise to the formation of **1**. Therefore if a mixture of both compounds (**1** and **1a**) is obtained, **1a** is not transformed into **1** by reaction with mPTA(OSO_2CF_3). Dependence of reaction products on the reactant concentration is not usual in chemical synthesis of ruthenium phosphine complexes. Theoretical and experimental studies aimed to elucidate the mechanism of the reaction between [RuClCp(PPh_3)$_2$] and mPTA are in progress and preliminary results were recently reported by the authors [13].

Slow evaporation of complex **1** in water solution enabled obtaining crystals of good quality. Monocrystal X-ray diffraction experiment confirmed the structure earlier proposed for this complex (*vide infra*) [7]. The stability of complex **1** and its behaviour in water at various pH were studied previously in order to evaluate its catalytic properties at pH 5.94, 2.17 and 11.56 as was monitored by UV–vis absorption spectroscopy. No change in **1** was observed at acidic pH while a net evolution was observed at basic pH [11].

A D_2O solution of **1** was prepared and several fractions of NaOH solution were added to it. The reaction was monitored by $^{31}P\{^1H\}$NMR spectroscopy. The spectra showed that the signal at −10.77 was decreasing while the one at −8.59 ppm (Fig. 1a) was increasing. The final compound was stable in solution for one day at room temperature. Addition of NaCl to the solution led to formation of complex **1** (Fig. 1b).

It is only possible to justify these results if one initially assumes that the Cl^- in [RuClCp(mPTA)$_2$](OSO_2CF_3)$_2$ (**1**) is substituted by OH^- giving rise to the complex [RuCp(OH-κ*O*)(mPTA)$_2$](OSO_2CF_3)$_2$·($C_4H_{10}O$) (**2**) in which the OH^- ligand is easily replaced by Cl^- bringing back the complex **1** (Scheme 2).

The complex **2** was isolated by precipitation with Et_2O from the reaction of **1** with NaOH in water. All our attempts to obtain good-quality monocrystals of **2** for X-ray diffraction experiment were unsuccessful. To support the proposed structure of **2** a lot of effort has been invested in obtaining the parent water complex [RuCp (mPTA)$_2$(OH_2-κ*O*)](OSO_2CF_3)$_3$·(H_2O)($C_4H_{10}O$)$_{0.5}$ (**3**), which was finally isolated by precipitation with Et_2O from the reaction of **1** with $AgOSO_2CF_3$ in water. It is important to point out that complex **3** transforms into **2** by reaction with NaOH in water, which supports the composition proposed for **2** and provides more convenient procedure for its synthesis (Scheme 3).

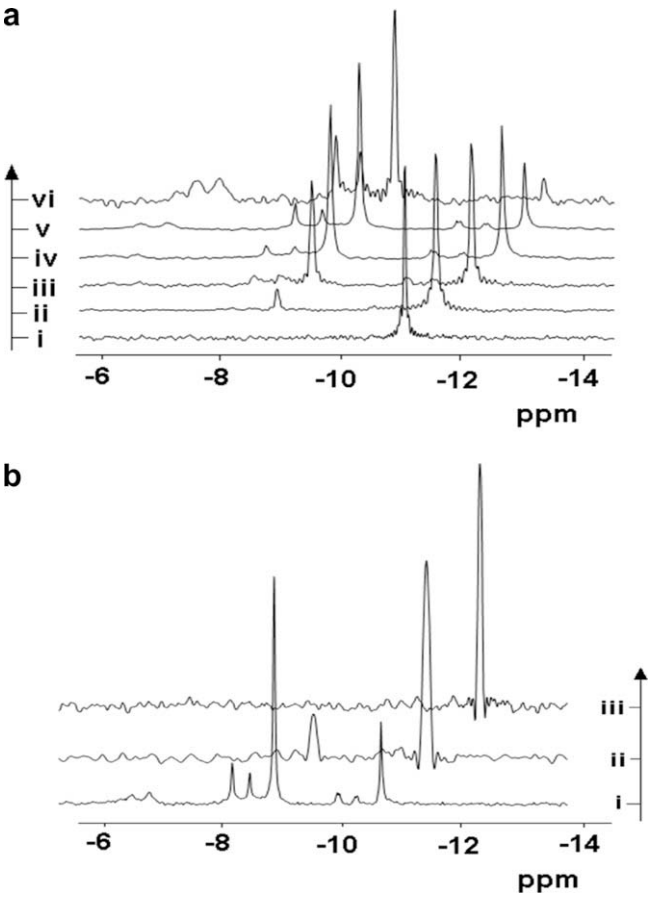

Fig. 1. (a) (i) $^{31}P\{^1H\}$ NMR (D_2O) of an aqueous solution of [RuClCp(mPTA)$_2$]-(OSO_2CF_3)$_2$ (**1**) (−10.77 ppm) was reacted with successive addition of (ii) 50 μL, (iii) 100 μL, (iv) 100 μL, (v) 150 μL and (vi) 300 μL of NaOH in water (0.075 M) at 298 K, leading to the conversion of **1** (−10.77 ppm) into **2** (−8.59 ppm). (b) $^{31}P\{^1H\}$ NMR (D_2O) of the solution obtained after successive addition of (ii) 25 μL, (iii) 125 μL of NaCl (0.35 M) into the resulting (a) solution (i) leading to the conversion of **2** (−8.59 ppm) into **1** (−10.77 ppm).

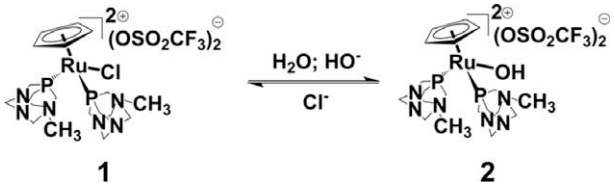

Scheme 2. Transformation of **1** into **2** in water solution.

The $^{19}F\{^1H\}$ NMR spectrum of **3** shows a unique singlet at −78.72 ppm which is similar to that observed for complex **1** (−78.84 ppm) and agrees well with the presence of an ionic $^-OSO_2CF_3$ molecule [7]. The same signal can be observed also if a large molar excess of $AgOSO_2CF_3$ is introduced in the reaction, indicating that there is no significant interaction between the metal and the anion $^-OSO_2CF_3$ (Scheme 3). The IR spectra of both complexes show O–H characteristic bands and their ^1H NMR and ^{13}C NMR (D_2O) display typical signals for diethyl ether molecules (*vide infra*).

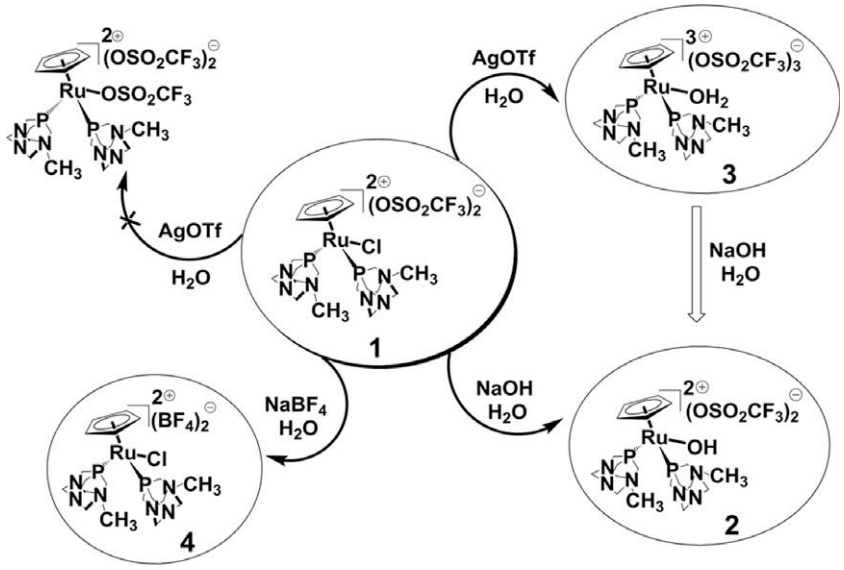

Scheme 3. Reactivity of **1** in water. Synthesis of **2**, **3** and **4**.

To confirm that assumption the complex $[RuClCp(mPTA)_2](BF_4)_2$ (**4**) was obtained by reaction of **1** with $NaBF_4$ in water at room temperature. The resulting orange solid showed similar ^1H and $^{31}P\{^1H\}$ NMR spectra as those for **1**.

However in its $^{19}F\{^1H\}$ NMR spectrum a multiplet at −147.90 ppm was observed which could only be assigned to an ionic BF_4^- molecule. The $^{31}P\{^1H\}$ NMR spectrum of **3** in D_2O shows a singlet at −10.69 ppm which is somewhat different from that of **1** (−10.77 ppm) but clearly different from that observed for **2** (−8.59 ppm). A $^{31}P\{^1H\}$ spectroscopy study of the reaction of **1** with $AgOSO_2CF_3$ in D_2O showed that the signal for **1** was slowly transformed into the one observed for **3** as was precipitating quantitatively AgCl (Fig. 2).

The spectroscopic properties of **3** support the conclusion that the H_2O molecule is coordinated to the metal. Stable ruthenium complexes containing water are not very common as strong atom like O-bonds weakly bound soft atoms like the Ru(II). There are two structurally characterised examples of mPTA–Ru complexes containing a H_2O ligand: the complex $[Ru(H_2O)_2(mPTA)_4]^{6+}$ [14] in which all water molecules are in *trans* position to each other, and the complex (OC-6-13)-$[RuI_2(H_2O)(mPTA)_3]I_3$ in which one mPTA is in *trans* position to the H_2O molecule [15]. There are no data concerning the crystal structure of Cp–mPTA–Ru complex, that contains the H_2O molecule coordinated to the metal [16]. However it is known that in water solution exists a partial equilibrium between the complex $[CpRuCl(PTA)_2]$ and its water parent complex $[CpRu(OH_2)(PTA)_2]^+$ [17].

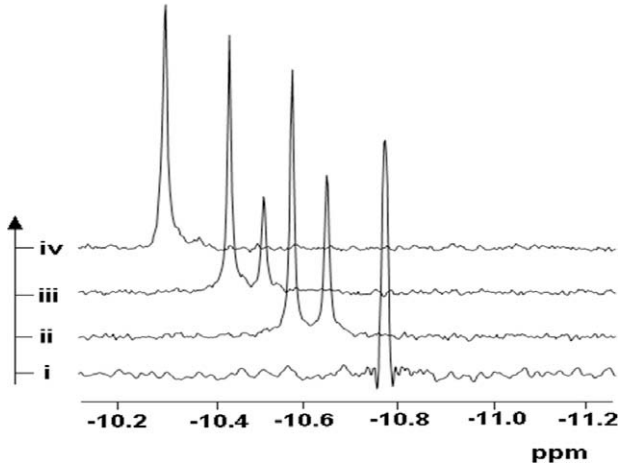

Fig. 2. (i) $^{31}P\{^1H\}$ NMR (D_2O) spectrum for the transformation of $[RuClCp(mPTA)_2](OSO_2CF_3)_2$ (**1**) (−10.77 ppm) in $[RuCp(mPTA)_2(OH_2\text{-}\kappa O)](OSO_2CF_3)_3\cdot(H_2O)(C_4H_{10}O)_{0.5}$ (**3**) (−10.69 ppm) by gently addition of (ii) 2 mg, (iii) 0.6 mg and (iv) 0.8 mg of solid AgOTf.

To have additional information to support the composition of complexes **2** and **3** a thermogravimetric study in nitrogen atmosphere was performed for both compounds as well as for the complex **1** for comparison purposes. Thermal data of the weight loss for **1–3** complexes are displayed in Table 1.

Complex **1** has high thermal stability from 25 to ca. 215 °C while complexes **2** and **3** decompose at 150 °C (Table 1). The TG-DTG/DTA curves (Fig. 3) for **2** and **3** reveal a first weight loss with three overlapped stages (see DTG curves), which is likely due to the loss of H_2O and Et_2O molecules. In fact, the temperature range where the first weight loss step occurs agrees well with the data on other compounds containing solvated and coordinated water molecules [18] and solvated diethyl ether molecules [19]. The loss of mass in this process (Table 1) indicates that one H_2O molecule and one Et_2O molecule are bound in complex **2** and two H_2O molecules and a half of Et_2O molecule are included in complex **3**.

Two simultaneous endothermic peaks at 112 and 138 °C are observed for **3** and one endothermic peak at 145 °C for **2**, which is in agreement with the fact that Ru–OH bond is stronger than Ru–OH_2 bond. At 215 °C the complex **1** decomposes with a endothermic peak at 230 °C ($[DTG]_{peak}$ c.a. 232 °C) while complex **2** and **3** show a continuous weight loss.

To obtain an improved procedure for obtaining complexes **2** and **3** a new synthetic route was planned (Scheme 4).

Complex **1** is soluble and stable in DMSO (70 mg/mL at 288 K) but the product of the reaction of **1** with $AgOSO_2CF_3$ in DMSO crystallises with a good yield. The ^1H, $^{13}C\{^1H\}$, $^{31}P\{^1H\}$ NMR spectroscopy show signals in similar range for mPTA and Cp ligands as those found in other parents mPTA–Ru complexes [7]. It is important to stress that signals for coordinated DMSO are observed at 2.54 and 39.88 ppm in ^1H NMR and $^{13}C\{^1H\}$ NMR, respectively. The $^{19}F\{^1H\}$ NMR spectrum reveals a singlet at −77.74 ppm which is in agreement with a ionic $^-OSO_2CF_3$ molecule [7]. The $^{31}P\{^1H\}$ NMR (D_2O) spectrum shows a single resonance at −12.73 ppm which is shifted ~2 ppm downfield from that observed for **1** and

Table 1
Thermal data of the complexes **1**–**3** from 25 to 250 °C.

Complexes	ΔT (°C)	$N^0_{molecules}$ losses	Calcd./found (%)	$[DTG]_{peak\ °C}$	$[DTA]_{peak\ °C}$
(**1**)	25–215	–	–	–	–
(**2**)	25–150	$(H_2O)_1$ and $(C_4H_{10}O)_{0.95}$	10.24/9.79	49, 125, 142	145
(**3**)	25–150	$(H_2O)_2$ and $(C_4H_{10}O)_{0.45}$	7.10/6.76	59, 112, 126	112, 138

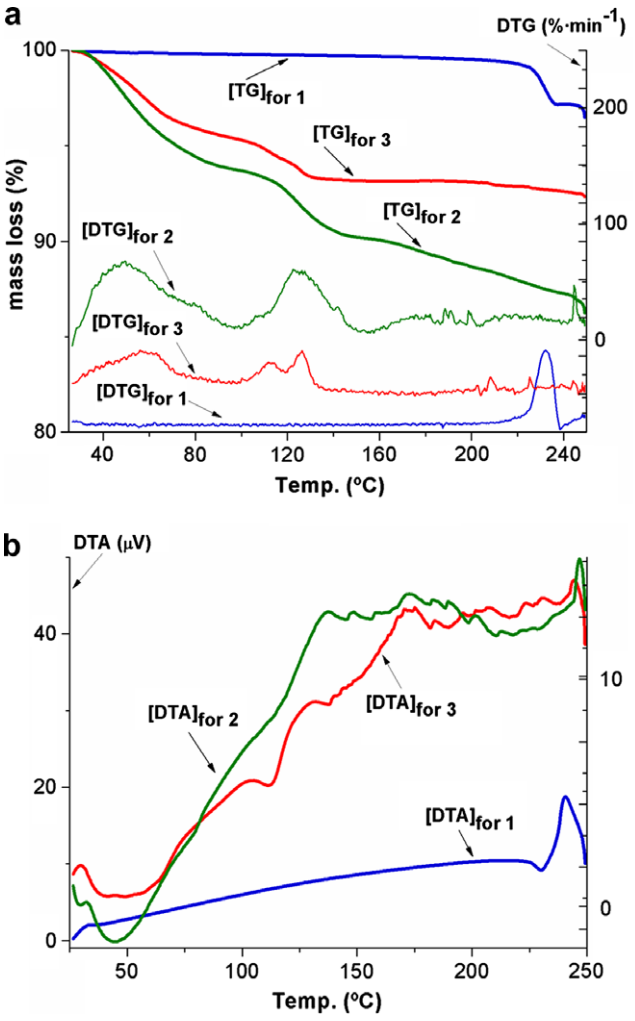

Fig. 3. (a) TG/DTG and (b) DTA curves of complexes **1**–**3**. TG = mass loss (%); (b) DTA = ΔT (microvolts; (↓ endo)) and DTG = percent per min.$^{-1}$.

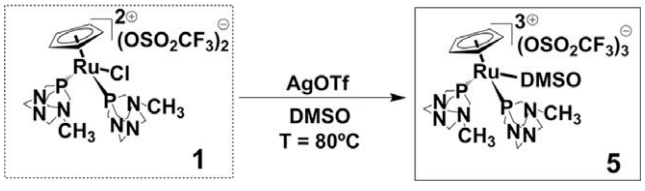

Scheme 4. Synthesis of **5**.

3 and ~4 ppm from that observed for **2**. Its spectroscopic properties support that the composition for the new complex is $[RuCp(DMSO\text{-}\kappa S)(mPTA)_2](OSO_2CF_3)_3$ (**5**), which was finally confirmed by single crystal X-ray determination. The exchange of the DMSO molecule by the H_2O molecule was tested by dissolution of **5** in water at room temperature. Neither after keeping **5** for 24 h at room temperature or after 72 h at 80 °C, no significant changes were detected by NMR, which demonstrates its high stability in water.

Complexes **2** and **3** are well soluble in water, dimethyl sulfoxide, less soluble in methanol and insoluble in diethyl ether. It is important to stress that the water solubility of complex **2** and **3** at 295 K (55 and 30.7 mg/mL, respectively), is larger than that for **1** (16 mg/mL). Both complexes, **2** and **3**, are stable enough in water but exchange easily the OH^- and H_2O ligand bonded to the metal, therefore they both are good candidates to mediate catalytic processes in water. Further experiments to determine the catalytic properties of complexes **1**, **2** and **3** in water for the isomerization of enols are in progress [11].

2.2. Structures of $[RuClCp(mPTA)_2](OSO_2CF_3)_2$ (**1**) and $[RuCp(DMSO\text{-}\kappa S)(mPTA)_2](OSO_2CF_3)_3\ 2H_2O$ (**5**)

Crystals good enough to be used for X-ray structure determination of **1** and **5** were obtained from an acetone and water solution by slow evaporation at room temperature. Both compounds crystallized in the monoclinic space group (Table 2) and the perspective drawing of their crystal structures along with the atom numbering depicted in Fig. 4. A comparison of the structures of **1** and **5** with related $[RuCp'X(L)(L')]^{n+}$ complexes ($Cp' = {}^5\eta\text{-}C_5H_5^-$, Cp; ${}^5\eta\text{-}C_8H_9^-$, Dp; ${}^5\eta\text{-}Me_5C_5^-$, Cp*; X = Cl, I, H, L = L' = PPh_3, PTA, mPTA) [3,7,8] reveals no major differences.

The Cp rings for the two complexes are essentially planar, the biggest separation being 0.0009 (C23) for **1** and 0.0345 Å (C5) for **5**, from overall plan for the Cp bonded to Ru1. The angle between the Cp_{cent} plane and the P1–Ru1–P2 plane was found to be 61.15(11)° for **1**, which is c.a. 9° greater than that found for **5**. These results are consistent with the values reported for similar piano-stool complexes (range 51.4–72.7°, mean 59.2°) [3,8]. The Ru1–Cp_{cent} distance is 1.840 for **1** and 1.883 Å for **5**, which are consistent with a Ru–Cp_{cent} bond length found in bibliography (range 1.836–1.929 Å, mean 1.893 Å) [3,7,8]. The P1–Ru1–P2 angle is

Table 2
Crystallographic data of complexes **1** and **5**.

	1	**5**
Formula	$C_{21}H_{35}N_6F_6ClO_6P_2S_2Ru$	$C_{24}H_{45}N_6F_9O_{12}P_2RuS_4$
Fw	844.13	1071.91
Crystal system	Monoclinic	Monoclinic
Space group	*P*2(1)/*c*	*P*2(1)/*n*
a (Å)	6.5110(2)	15.225(2)
b (Å)	20.3062(7)	11.407(5)
c (Å)	23.2101(8)	23.551(3)
α (°)	90.00	90.00
β (°)	90.480(1)	90.01(3)
γ (°)	90.00	90.00
V (Å^3)	3068.58(18)	4090.1(19)
Z	4	4
$d_{calcd.}$ (g cm^{-3})	1.827	1.687
Absorption coefficient (mm^{-1})	0.924	0.764
Data/restrains/parameters	5408/0/408	9734/0/502
Final *R* indices [$I > 2\sigma(I)$]	$R_1 = 0.0504$; $wR_2 = 0.1294$	$R_1 = 0.0763$; $wR_2 = 0.2061$
R indices (all data)	$R_1 = 0.0570$; $wR_2 = 0.1439$	$R_1 = 0.1060$; $wR_2 = 0.2337$
Largest diffraction peak, hole (e Å^3)	1.134; −1.088	2.567; −0.975

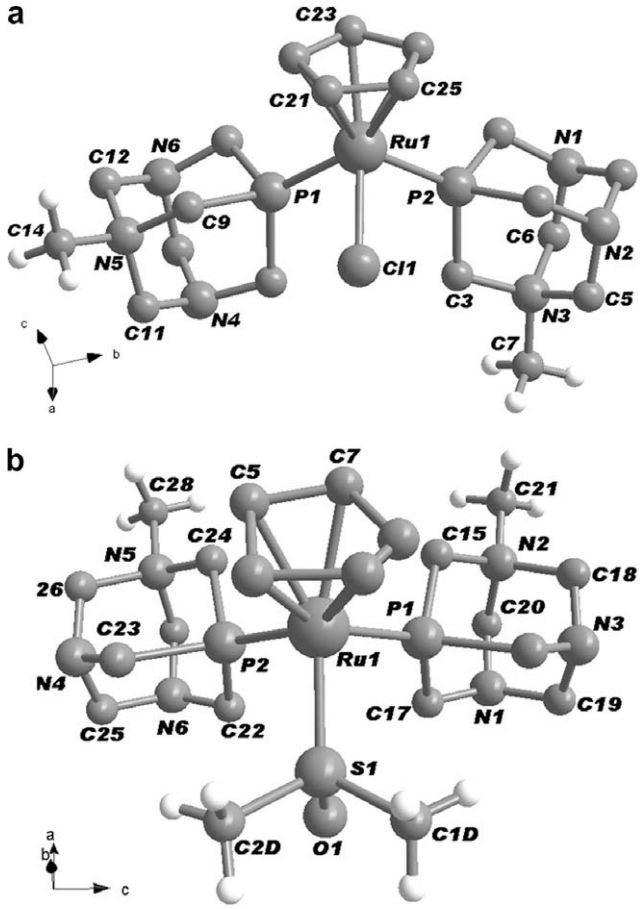

Fig. 4. Complex unit structure of (a) $[RuClCp(mPTA)_2]^{2+}$and (b) $[RuCp(DMSO\text{-}kS)(mPTA)_2]^{3+}$ including the atomic numbering scheme. For clarity, only methyl hydrogen atoms are included.

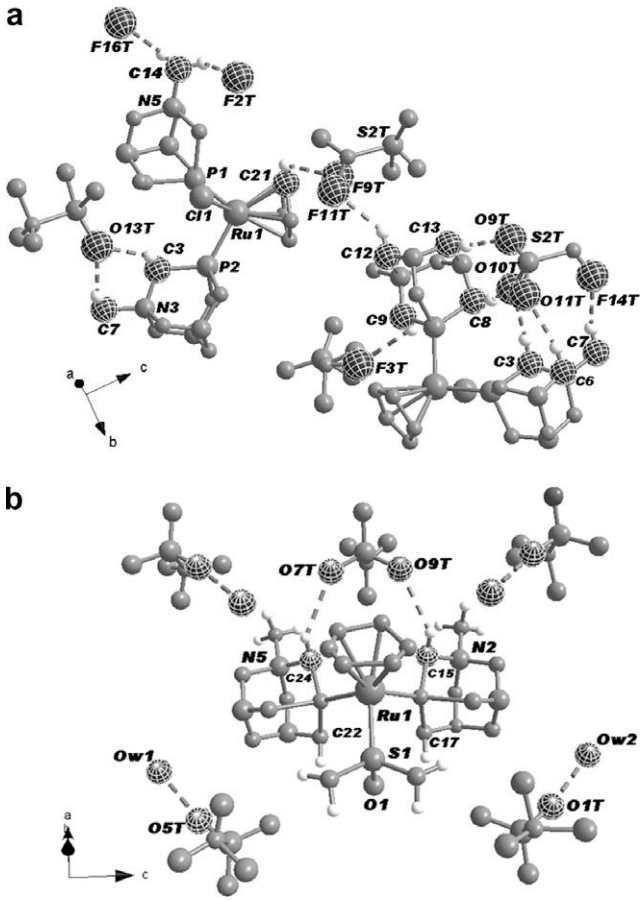

Fig. 5. Packing for **1** (a) and **5** (b), including the atomic numbering scheme. Dashed lines represent the selected intermolecular interactions (the O and F atoms design are in globe stile).

Table 3
Selected bond lengths (Å) and angles (°) for **1** and **5**.

1		5	
Ru1–P1	2.2509(12)	Ru1–P1	2.2927(16)
Ru1–P2	2.2599(12)	Ru1–P2	2.2930(16)
Ru1–Cl1	2.4213(13)	Ru1–S1	2.2632(15)
P1–Ru1–P2	99.44(4)	P1–Ru1–P2	97.41(6)
P1–Ru1–Cl1	84.55(5)	P1–Ru1–S1	90.83(6)
P2–Ru1–Cl1	87.04(5)	P2–Ru1–S1	90.78(6)

99.94(4)° in **1**, which is slightly higher than in **5** (97.41(6)°) and virtually identical to those found for the analogue in the ruthenium complexes (range 93.20(2)–100.12(8)° (mean 97.67(6)°) [3,7,8]. As shown in Table 3, other bond distances and angles fall well in the range of values reported in literature [3,7,8,20]. Finally, for both complexes (Fig. 4), the carbon–nitrogen bond distances (N)C–N corresponding to the nitrogen supporting methyl group (N3/N5 for **1** and N2/N5 for **5**) are longer (range 1.503(8)–1.543(8) Å) than those for the non-substituted nitrogen atoms (range 1.405(9)–1.481(11) Å). These values are in agreement with those found for dmoPTA in the cation unit $[RuClCp(PPh_3)(HdmoPTA]^+$ [8a].

The crystal packing diagram (Fig. 5) shows an extensive weak intermolecular interaction among the molecules that provides an additional stabilization for the structures of the two complexes [21]. In complex **1**, relatively strong C···O separation is observed within standard hydrogen bonding distances: C7···O13T (C7-H7C···O13T = 2.018(2) Å; H7C···O13T = 2.840(5) Å; Ĥ = 142.5(6)°, $1-x$, $1-y$, $1-z$).

Similarly, in complex **5** the O_w···O distances are coherent with hydrogen bond: O_{w1}/O_{w2}···O5T/O1T = 3.046(4)–3.033(3) Å [21].

3. Experimental

3.1. Materials

All chemicals were reagent grade and, unless otherwise stated, used as received by commercial suppliers. Likewise all reactions were carried out under a pure argon atmosphere in freshly distilled and oxygen-free solvents using standard Schlenk-tube techniques. The hydrosoluble phosphines $[RuClCp(PPh_3)_2]$ and $[RuClCp(PTA)_2]$ were prepared as described in the literature [7,12].

3.2. General physical methods

^1H and $^{13}C\{^1H\}$ NMR spectra were recorded at room temperature at 400.13 and 100.62 MHz, respectively, on a Bruker DRX400 instrument. Peak positions are relative to tetramethylsilane and were calibrated against the residual solvent resonance (^1H) or the deuterated solvent multiplet (^{13}C). $^{31}P\{^1H\}$ NMR spectra were recorded on the same instrument operating at 161.97 MHz and the chemical shifts for $^{31}P\{^1H\}$ NMR were measured relative to external 85% H_3PO_4. $^{19}F\{^1H\}$ NMR spectra were recorded on the same instrument operating at 376.45 MHz. Infrared spectra were recorded as KBr disks using a ThermoNicolet Avatar 360 FT-IR spectrometer. Elemental analyses (C, H, N and S) were performed on a Fisons Instrument EA 1108 elemental analyzer. Thermal analyses were carried out on a Perkin-Elmer system (mod. Pyris Diamond TG/DTA) under a nitrogen

atmosphere (flow rate: 80 cm^3 min^{-1}) from 25 to 250 °C. The samples (ca. 10 mg) were heated in an aluminium crucible (45 mL) at a rate of 5°C min^{-1}. The TG curves were analysed as mass loss (milligrams) as a function of temperature. The number of decomposition steps was identified in derivative thermogravimetric curves (DTG). The endo and exo thermal processes were identified by use of differential thermal analysis curves (DTA).

3.3. Preparation of $[RuClCp(mPTA)_2](OSO_2CF_3)_2$ (**1**)

The compound was prepared by two alternative processes:

(A) The compound $CH_3OSO_2CF_3$ (0.081 mL, 0.73 mmol) was added via a syringe to a solution of $[RuClCp(PTA)_2]$ (0.31 g, 0.60 mmol) in 45 mL of chloroform at reflux and kept for 2 h. The resulting yellow precipitate was filtered, washed with Et_2O (2 × 3 mL) and vacuum-dried.

(B) To a vigorously stirred solution of $[RuClCp(PPh_3)_2]$ (1 g, 1.38 mmol) in 200 mL of acetone mPTA(OSO_2CF_3) (0.98 g, 3.05 mmol) was added. Slowly a yellow precipitate was formed. After 4 h. the resulting powder was collected by filtration, washed with Et_2O (2 × 5 mL) and vacuum-dried.

Yield: (A) 0.23 g, 74%; (B) 0.65 g, 64%. S_{25°,H_2O} = 16 mg/mL, $S_{22\ ^\circ C,DMSO}$ = 70 mg/mL. $^{31}P\{^1H\}$ NMR(DMSO-d_6): δ −8.57 (s, mPTA). Characterisation data agree with those reported [7].

3.4. Reaction of $[RuClCp(PPh_3)_2]$ with mPTA(OSO_2CF_3) vs. acetone volume

Reactions were performed by a similar procedure as described previously for the synthesis of **1** (method B) but solvent volume was modified. Two solutions of $[RuClCp(PPh_3)_2]$ (0.1 g, 0.14 mmol) and mPTA(OSO_2CF_3) (0.09 g, 0.28 mmol) in acetone volume (*a*) = 10 mL and (*b*) = 25 mL, were refluxed for 4 h. The precipitates obtained (*i*) as an orange powder and *(ii)* as a yellow-powder, were filtered under Ar, washed with Et_2O (2 × 2 mL) and vacuum-dried. *Experiment* (*a, orange-powder*): $^{31}P\{^1H\}$ NMR(DMSO-d_6): δ −15.56 (d, $^2J_{PP}$ = 54.81 Hz, mPTA) and 47.25 (d, $^2J_{PP}$ = 54.81 Hz, PPh_3) (which were assigned to $[RuClCp(mPTA)(PPh_3)](OSO_2CF_3)$ (**1a**) [7]); −8.57 (s, mPTA) (**1**) (ratio **1a**:**1** = 67:33%). *Experiment* (*b, yellow-powder*): $^{31}P\{^1H\}$ NMR(DMSO-d_6): δ −8.57 (s, mPTA) (**1**) (ratio **1a**:**1** = 0:100%).

3.5. Reaction of $[RuClCp(mPTA)(PPh_3)](OSO_2CF_3)$ (**1a**) with mPTA(OSO_2CF_3)

Complex **1a** (100 mg, 0.13 mmol) was added to mPTA(OSO_2CF_3) (49 mg, 0.15 mmol) dissolved in acetone (25 mL) and the mixture was refluxed for 4 h. The precipitate obtained was filtered, washed with Et_2O (2 × 2 mL) and vacuum-dried, and the filtered liquor was evaporated. Both solids were analysed by $^{31}P\{^1H\}$ NMR which showed that only **1a** and mPTA(OSO_2CF_3) were isolated from the reaction.

3.6. Reaction of **1** with NaOH

The complex **1** (9.5 mg, 0.011 mmol) was dissolved in 0.7 mL of D_2O in a 5 mm NMR tube. The resulting solution was charged with successive additions of 50, 100, 100, 150 and 300 μL of NaOH (0.075 M) at 298 K, leading to conversion of **1** into **2** to ~11%, 42%, 66%, 75% and 89%.

3.7. Preparation of $[RuCp(mPTA)_2(OH_2\text{-}\kappa O)](OSO_2CF_3)_3\cdot(H_2O)(C_4H_{10}O)_{0.5}$ (**3**)

Complex **1** (200 mg, 0.24 mmol) dissolved in water (20 mL) was added to $AgOSO_2CF_3$ (82 mg, 0.32 mmol) dissolved in water (1.2 mL) and the mixture was stirred for 4 h at room temperature. The solution was then filtered several times through Celite to remove the AgCl precipitate and was dried under vacuum. The oily residue was triturated with Et_2O (8 × 5 mL) and the resulting yellow-orange powder was dried in vacuum.

Yield: 141.8 mg, 70.1%. $C_{24}H_{44}N_6F_9O_{11.5}P_2RuS_3$ (1030.84 g/mol): calcd. C 27.98, H 4.26, N 8.15, S 9.31. Found C 28.01, H 4.17, N 8.20; S 9.25%. $S_{22^\circ C,H_2O}$ = 55 mg/mL; $S_{22\ ^\circ C,DMSO}$ = 98.33 mg/mL; $S_{22^\circ\ C,CH_3OH}$ = 5.8 mg/mL. IR (KBr, cm^{-1}): $\nu_{(OTf)}$ 1239, $\nu_{(H_2O)}$ 3459, 3357. ^1H NMR (D_2O): δ 1.11 (t, CH_3, ether), 2.85 (s, NCH_3, 6H), 3.49 (q, CH_2, ether), 3.99–4.20 (m, NCH_2P, 8H), 4.46–4.61 (m, NCH_2 N + PCH_2NCH_3, 8H), 4.90 (s, C_5H_5, 5H). 4.94–5.08 (m, NCH_2NCH_3, 8H). $^{13}C\{^1H\}$ NMR (D_2O): δ 14.54 (s, CH_3, ether), 49.72 (s, CH_3 N), 51.08 (bd, $^1J_{CP}$ = 37.92 Hz, NCH_2P), 52.19 (bd, $^1J_{CP}$ = 32.32 Hz, NCH_2P), 60.04 (bd, $^1J_{CP}$ = 21.08 Hz, CH_3NCH_2P), 66.42 (s, CH_2, ether), 69.35 (s, NCH_2 N), 77.74 (s, CH_3NCH_2 N), 80.71 (s, C_5H_5), 120.10 (q, $^1J_{CF}$ = 315. 19 Hz, OSO_2CF_3). $^{31}P\{^1H\}$ NMR (D_2O): δ −10.69 (s). $^{19}F\{^1H\}$ NMR (D_2O): δ −78.72 (s, OSO_2CF_3).

3.8. Preparation of $[RuCp(OH\text{-}\kappa O)(mPTA)_2](OSO_2CF_3)_2\cdot(C_4H_{10}O)$ (**2**)

(A) NaOH (6 mg, 0.15 mmol) was added to complex **1** (90.5 mg, 0.11 mmol) dissolved in water (6 mL) and the mixture was stirred for 1 h at room temperature. The solution was filtered under Ar and dried under vacuum. The oily residue triturated with with Et_2O (8 × 5 mL) and the resulting powder dried in vacuum.

(B) NaOH (1.72 mg, 0.043 mmol) was added to complex **3** (42 mg, 0.041 mmol) dissolved in water (6 mL) and the mixture was stirred for 1 h at room temperature. The solution was filtered under Ar and dried under vacuum. The oily residue was triturated with Et_2O (8 × 5 mL) and the resulting powder dried in vacuum.

Yield: (A) 46.3 mg, 48% (B) 32.30 mg, 76.90%. $C_{25}H_{46}N_6F_6O_8P_2RuS_2$ (899.80 g/mol): calcd. C 33.34, H 5.11, N 7.11, S 9.34. Found C 33.12, H 5.14, N 7.20; S 9.12%. $S_{22^\circ C,H_2O}$ = 30.7 mg/mL; $S_{22\ ^\circ C,DMSO}$ = 62.7 mg/mL; $S_{22^\circ C,CH_3OH}$ = 19.2 mg/mL . IR (KBr, cm^{-1}): $\nu_{(OTf)}$ 1239, $\nu_{(H_2O)}$ 3533, 3514. ^1H NMR (D_2O): δ 1.11 (t, CH_3, ether), 2.84 (s, NCH_3, 6H), 3.49 (q, CH_2, ether), 3.98–4.17 (m, NCH_2P, 8H), 4.44–4.63 (m, NCH_2 N + PCH_2NCH_3, 8H), 4.85 (s, C_5H_5, 5H). 4.93–5.03 (m, NCH_2NCH_3, 8H). $^{13}C\{^1H\}$ NMR (D_2O): δ 14.53 (s, CH_3, ether), 49.64 (s, CH_3 N), 51.41 (bd, $^1J_{CP}$ = 26.72 Hz, NCH_2P), 52.64 (bd, $^1J_{CP}$ = 35.12 Hz, NCH_2P), 60.44 (bd, $^1J_{CP}$ = 15.44 Hz, CH_3NCH_2P), 66.54 (s, CH_2, ether), 69.31 (s, NCH_2 N), 78.24 (s, CH_3NCH_2 N), 80.58 (s, C_5H_5), 120.22 (q, $^1J_{CF}$ = 374. 75 Hz, OSO_2CF_3). $^{31}P\{^1H\}$ NMR (D_2O): δ −8.59 (s). $^{19}F\{^1H\}$ NMR (D_2O): δ −78.77 (s, OSO_2CF_3).

3.9. Reaction of **2** with NaCl

The complex **2** (8.0 mg, 0.009 mmol) was dissolved in 0.6 mL of D_2O in a 5 mm NMR tube. The resulting solution was charged with successive additions of 25, 125 μL of NaCl (0.35 M), leading to conversion of **2** into **1** to 70 and 100%.

3.10. Preparation of $[RuClCp(mPTA)_2](BF_4)_2$ (**4**)

$NaBF_4$ (68 mg, 0.62 mmol) was added to complex **1** (100 mg, 0.12 mmol) dissolved in water (5 mL) and the mixture was stirred for 25 min. at room temperature. The resulting orange precipitate was filtered, washed with Et_2O (2 × 2 mL) and vacuum-dried.

Yield: 72.8 mg, 73%. $S_{22^\circ\ C,H_2O}$ = 0.29 mg/mL; $S_{22\ ^\circ C,DMSO}$ = 15 mg/mL. $C_{19}H_{35}N_6P_2F_8B_2RuCl$ (719.60 g/mol): calcd. C 31.71, H 4.86, N 11.67. Found C 31.68, H 4.82, N 11.93%. IR (KBr, cm^{-1}): $\nu_{(BF_4)}$ 1035. NMR spectrum are identical to that found for 1 with

exception of $^{-}OSO_2CF_3$ carbon signal in $^{13}C\{^1H\}$ NMR. ^{19}F NMR (DMSO-d_6): δ 147.90 (m, BF_4).

3.11. Reaction of **1** with AgTOf

Into a NMR 5 mm tube 1 (9.5 mg, 0.011 mmol), 0.8 mL of D_2O were introduced and 3.4 mg of solid $AgOSO_2CF_3$ (0.015 mmol) was gently added to the water solution. Slowly an AgCl precipitate was separated, leading to ~58%, 70% and 100% conversion into **3**.

3.12. Preparation of [RuCp(DMSO-κS) (mPTA)$_2$](OSO$_2$CF$_3$)$_3$ 2H$_2$O (**5**)

$AgOSO_2CF_3$ (45.7 mg, 0.18 mmol) dissolved in DMSO (2 mL) was added to complex 1 (100 mg, 0.12 mmol) dissolved in DMSO (2 mL) and the mixture was stirred for 17 h at 80 °C and filtered under vacuum. After addition of Et_2O (6x15 mL) a light yellow precipitate was obtained which was vacuum-dried. Crystals good enough for X-ray determination were obtained by slow evaporation from a water solution.

Yield: 96.5 mg, 76.0%. $C_{24}H_{45}N_6F_9O_{12}P_2RuS_4$ (1071.91 g/mol): calcd. C 26.86, H 4.20, N 7.84, S 11.96. Found C 26.89, H 4.10, N 7.67 S 11.52%. IR (KBr, cm^{-1}): $\nu_{(OTf)}$ 1257, 1061, $\nu_{(S=O)}$ (DMSO-S)1025. ^1H NMR (DMSO-d_6): δ 2.54 (s, DMSO-S, 6H), 2.78 (s, NCH_3, 6H), 3.91–4.17 (m, NCH_2P, 8H), 4.33–4.77 (m, NCH_2 N + PCH_2NCH_3, 8H), 4.95–5.22 (m, NCH_2NCH_3, 8H), 5.50 (s, C_5H_5, 5H). $^{13}C\{^1H\}$ NMR (DMSO-d_6): δ 39.88 (CH_3, DMSO-S), 48.90 (s, CH_3 N), 52.17 (bd, $^1J_{CP}$ = 34.62 Hz, NCH_2P), 53.02 (bd, $^1J_{CP}$ = 39.42 Hz, NCH_2P), 59.88 (bd, $^1J_{CP}$ = 25.68 Hz, CH_3NCH_2P), 68.38 (s, NCH_2 N), 79.53 (s, CH_3NCH_2 N), 84.55 (s, C_5H_5), 121.04 (q, $^1J_{CF}$ = 320. 15 Hz, OSO_2CF_3). $^{31}P\{^1H\}$ NMR (DMSO-d_6): δ −11.25 (s). $^{19}F\{^1H\}$ NMR (DMSO-d_6): δ −77.74 (s, OSO_2CF_3). ^1H NMR (D_2O): δ 2.85 (s, NCH_3, 6H), 3.43 (s, DMSO-S, 6H), 4.01–4.27 (m, NCH_2P, 8H), 4.41–4.62 (m, NCH_2 N + PCH_2NCH_3, 8H), 4.93–5.13 (m, NCH_2NCH_3, 8H), 5.36 (s, C_5H_5, 5H).$^{13}C\{^1H\}$ NMR (D_2O): δ 39.88 (m, $(CH_3)_2SO$), 49.08 (s, CH_3 N), 52.28 (bd, $^1J_{CP}$ = 37.23 Hz, NCH_2P), 52.68 (bd, $^1J_{CP}$ = 36.60 Hz, NCH_2P), 57.63 (CH_3, DMSO-S), 60.14 (bd, $^1J_{CP}$ = 26.14 Hz, CH_3NCH_2P), 68.61 (s, NCH_2 N), 80.03 (s, CH_3NCH_2 N), 84.23 (s, C_5H_5), 119.54 (q, $^1J_{CF}$ = 315. 05 Hz, OSO_2CF_3). $^{31}P\{^1H\}$ NMR (D_2O): δ −12.73 (s).

3.13. Stability of 5 in water

The compound 5 (15 mg, 0.015 mmol) was dissolved in 0.5 mL of D_2O in a 5 mm NMR tube. No significant changes were observed after 10 min at room temperature, 2 h at 40 °C and 72 h at 80 °C.

3.14. Crystallographic data collection and structures determination

Single crystals of compound **1** and **5** were mounted on a glass fibre with epoxy cement at room temperature. Crystal data and data collection details are given in Table 2. Data collection for **1** was performed on a Bruker APEX CCD diffractometer (XDIFRACT service of the University of Almeria) in the range of $1.33 \leqslant 2\theta \leqslant 25.04$. Data were collected at 273(2) K, using graphite-monochromatized Mo Kα radiation (λ = 0.71073 Å).The usual corrections were applied to 16431 reflections collected, of which 4797 were unique with $I_0 > 2\sigma(I_0)$. Data collection for **5** was performed on a KappaCCD diffractometer (XDIFRACT service of the University of La Laguna) in the range of $1.59 \leqslant 2\theta \leqslant 28.65$. Data were collected at 293(2) K, using graphite-monochromatized Mo Kα radiation (λ = 0.71070 Å). Lorentz and polarisation corrections were applied to 24,620 reflections collected, of which 7122 were unique with $I_0 > 2\sigma(I_0)$. Both structures were determined by direct methods (SIR97 [22] or SHELXS-XTL [23]) and refined by least-squares procedures on F^2 (SHELXXTL). The Cp ring in **5** and $^{-}OSO_2CF_3$ anions in both complexes, were found to be disordered and refined isotropically. All non-hydrogen non-disordered atoms for the compounds were refined anisotropically. The function minimised during the refinement was $w = 1/[\sigma^2(F_0^2) + (0.0700P)^2 + 11.4777P]$ for **1** and $w = 1/[\sigma^2(F_0^2) + (0.1186P)^2 + 10.5715P]$ for **5.** The final geometrical calculations and the graphical manipulations were carried out with the SHELXS-XTL package [23].

4. Conclusions

Investigation of the behaviour of complex **1** in aqueous solution in the acidic/basic medium showed no significant spectral changes over time in acidic medium, however in a basic medium complex **1** transforms to the hydroxyl complex [RuCp(OH-κ*O*)(mPTA)$_2$](O-SO$_2$CF$_3$)$_2$·(C$_4$H$_{10}$O) (**2**). This process is reversible as addition of ionic chloride into a water solution of **2** led to **1**. Complex [RuCp-(mPTA)$_2$(OH$_2$-κ*O*)](OSO$_2$CF$_3$)$_3$·(H$_2$O)(C$_4$H$_{10}$O)$_{0.5}$ (**3**) was obtained from **1** by reaction with Ag(OSO$_2$CF$_3$) in water solution. Complex **2** is also obtained by reaction of **3** with OH^-. Substitution reaction of the Cl^- bonded to the metal in **1** by DMSO leads to [RuCp(DMSO-κ*S*)(mPTA)$_2$](OSO$_2$CF$_3$)$_3$ 2H$_2$O (**5**) which is very stable in solid state and water solution. The high aqua-solubility and the observed easy exchange of the OH and OH_2 ligand at 288 K in **2** and **3** make these complexes good candidates for being studied as catalytic species in water.

Acknowledgments

Funding is provided by Junta de Andalucía through PAI (research teams FQM-317) and Excellence Projects FQM-03092, and the MCYT (Spain) projects CTQ2006-06552/BQU. We also thank the Consejería de Educación, Cultura y Deportes (Gobierno Autónomo de Canarias, Spain), for supporting B. González.

References

[1] (a) B. Dutta, C. Scolaro, R. Scopelliti, P.J. Dyson, K. Severin, Organometallics 27 (2008) 1355;
(b) A. Romerosa, M. Saoud, T. Campos-Malpartida, C. Lidrissi, M. Serrano-Ruiz, M. Peruzzini, J.A. Garrido, F. García-Maroto, Eur. J. Inorg. Chem. 18 (2007) 2803;
(c) C. Lidrissi, A. Romerosa, M. Saoud, M. Serrano-Ruiz, L. Gonsalvi, M. Peruzzini, Angew. Chem., Int. Ed. 44 (2005) 2568.
[2] (a) T. Campos-Malpartida, M. Fekete, F. Joó, A. Kathó, A. Romerosa, M. Saoud, W. Wojtków, J. Organomet. Chem. 693 (2008) 468;
(b) D.A. Krosgstad, G.S. Ellis, A.K. Gunderson, A.J. Hammrich, J.W. Rudolf, J.A. Halfen, Polyhedron 26 (2007) 4093;
(c) F. Joó, Acc. Chem. Res. 35 (2002) 738.
[3] (a) C.A. Mebi, R.P. Nair, B.J. Frost, Organometallics 26 (2007) 429;
(b) B.J. Frost, C.A. Mebi, Organometallics 23 (2004) 5317.
[4] (a) M. Erlandsson, L. Gonsalvi, A. Ienco, M. Peruzzini, Inorg. Chem. 47 (2008) 8;
(b) M. Erlandsson, V.R. Landaeta, L. Gonsalvi, M. Peruzzini, A.D. Phillips, P.J. Dyson, G. Laurenczy, Eur. J. Inorg. Chem. 4 (2008) 620;
(c) L. Jaremko, A.M. Kirillov, P. Smolenski, T. Lis, A.J.L. Pombeiro, Inorg. Chem. 47 (2008) 2924;
(d) C.A. Vock, A.K. Renfrew, R. Scopelliti, L. Juillerat-Jeanneret, P.J. Dyson, Eur. J. Inorg. Chem. 10 (2008) 1661;
(e) M.P. Cifuentes, M.G. Humphrey, G.A. Koutsantonis, N.A. Lengkeek, S. Petrie, V. Sanford, P.A. Schauer, B.W. Skelton, R. Stanger, A.H. White, Organometallics 27 (2008) 1716;
(f) P. Bergamini, V. Bertolasi, L. Marvelli, A. Canella, R. Gavioli, N. Mantovani, S. Mañas, A. Romerosa, Inorg. Chem. 46 (2007) 4267.
[5] For a review on PTA chemistry, see A.D. Phillips, L. Gonsalvi, A. Romerosa, F. Vizza, M. Peruzzini, Coord. Chem. Rev. 248 (2004) 995.
[6] (a) G.W. Wong, W.-C. Lee, B.J. Frost, Inorg. Chem. 47 (2008) 612;
(b) R. Huang, B.J. Frost, Inorg. Chem. 46 (2007) 10962.
[7] A. Romerosa, T. Campos-Malpartida, C. Lidrissi, M. Saoud, M. Serrano-Ruiz, M. Peruzzini, J.A. Garrido-Cárdenas, F. García-Maroto, Inorg. Chem. 45 (2006) 1289.
[8] (a) A. Mena-Cruz, P. Lorenzo-Luis, A. Romerosa, M. Serrano-Ruiz, Inorg. Chem. 47 (2008) 2246;
(b) A. Mena-Cruz, P. Lorenzo-Luis, A. Romerosa, M. Saoud, M. Serrano-Ruiz, Inorg. Chem. 46 (2007) 6120.
[9] M. Serrano-Ruiz, A. Romerosa, B. Sierra-Martin, A. Fernandez-Barbero, Angew. Chem., Int. Ed. 47 (2008) 8665.

[10] S. Bolaño, L. Gonsalvi, F. Zanobini, F. Vizza, V. Bertolasi, A. Romerosa, M. Peruzzini, J. Mol. Cat. A: Chem. 224 (2004) 61.
[11] B. González, PhD Thesis in preparation, Department of Inorganic Chemistry, University of La Laguna, Canary Islands, Spain.
[12] D.N. Akbayeva, L. Gonsalvi, W. Oberhauser, M. Peruzzini, F. Vizza, P. Brüggeller, A. Romerosa, G. Sava, B.A. Bergamo, Chem. Commun. (2003) 264.
[13] B. Gonzalez, P. Lorenzo-Luis, A. Romerosa, M. Serrano-Ruiz, P. Gili, J. Mol. Struct. (THEOCHEM) 894 (2009) 59.
[14] J. Kovács, F. Joó, A. Bényei, G. Laurenzy, Dalton Trans. (2004) 2336.
[15] P. Smoleński, F.P. Pruchnik, Z. Ciunik, T. Lis, Inorg. Chem. 42 (2003) 3318.
[16] (a) Inorganic Crystal Structure Database (ICSD), Version 1.4.4, 2008-1.;
(b) X'Pert HighScore Plus Database, Version 2.2c (2.2.3) (2007), PANanlytical B.V., Almelo, The Netherlands, 2007.
[17] C.A. Mebi, P.N. Radhika, B.J. Frost, Organometallics 26 (2007) 429.
[18] (a) T. Bataille, F. Costantino, P. Lorenzo-Luis, S. Midollini, A. Orlandini, Inorg. Chim. Acta 362 (2008) 9;
(b) S. Ciattini, F. Constantino, P. Lorenzo-Luis, S. Midollini, A. Orlandini, A. Vacca, Inorg. Chem. 44 (2005) 4008.
[19] K. Melánová, L. Benes, V. Zima, M. Trchová, J. Dybal, Eur. J. Inorg. Chem. (2004) 2493.
[20] (a) W.-L. Man, H.-K. Kwong, W.W.Y. Lam, J. Xiang, T.-W. Wong, W.-H. Lam, W.-T. Wong, S.-M. Peng, T.-C. Lau, Inorg. Chem. 47 (2008) 5936;
(b) I. Bratsos, B. Serli, E. Zangrando, N. Katsaros, E. Alessio, Inorg. Chem. 46 (2007) 975;
(c) E. Alessio, G. Mestroni, G. Nardin, W.M. Attia, M. Calligaris, G. Save, S. Zorzet, Inorg. Chem. 27 (1988) 4099.
[21] (a) T. Steiner, Angew. Chem., Int. Ed. 41 (2002) 48;
(b) T. Steiner, G.R. Desiraju, Chem. Commun. (1998) 891;
(c) G.R. Desiraju, Acc. Chem. Res. 24 (1991) 290.
[22] A. Altamore, G. Cascarano, C. Giacovazzo, A. Guagliardi, G. Moliterni, M.C. Burla, G. Polidori, M. Camalli, R. Spagna, Sir 97 Package Program, 1997.
[23] G.M. Sheldrick, SHELXTL Version 6.14; Bruker-AXS Madison, WI, 2003.